



Contents lists available at ScienceDirect

Intermetallics

journal homepage: www.elsevier.com/locate/intermet

Critical assessment and thermodynamic modeling of the binary Mg–Zn, Ca–Zn and ternary Mg–Ca–Zn systems

S. Wasiur-Rahman, M. Medraj*

Department of Mechanical Engineering, Concordia University, 1455 De Maisonneuve Blvd. West, Montreal, QC, Canada H3G 1M8

ARTICLE INFO

Article history:

Received 28 October 2008

Received in revised form

7 January 2009

Accepted 16 March 2009

Available online xxx

Keywords:

A. Ternary alloy systems

B. Thermodynamic and thermochemical properties

E. Phase diagram, prediction

G. Automotive uses

ABSTRACT

Critical assessment of the experimental data and re-optimization of the binary Mg–Zn, Ca–Zn systems and the Laves phase of the Mg–Ca system have been performed. A comprehensive thermodynamic database of the Mg–Ca–Zn ternary system is presented. All available as well as reliable experimental data both for the thermodynamic properties and phase boundaries are reproduced within experimental error limits. In the present assessment, the Modified Quasichemical Model in the pair approximation is used for the liquid phase to account for the presence of the short-range ordering properly. The intermediate solid solutions are modeled using the compound energy formalism. Since the literature included contradicting information regarding the ternary compounds in this system, thermodynamic modeling of phase equilibria is used to determine the most likely description of this system and to exclude the self-contradicting experimental observations.

© 2009 Elsevier Ltd. All rights reserved.

1. Introduction

The main objective of adding alloying elements to pure magnesium is to increase the strength, corrosion and creep resistances which are important for industrial applications including automotive and aerospace sectors. It was found that alloying Mg with Ca increases the strength, castability and corrosion resistance whereas the presence of Zn in the binary Mg–Ca alloys enhances the precipitation hardening response [1]. As part of a broader research project to create a self-consistent database for the Mg alloys, a thermodynamic description of the Mg–Ca–Zn ternary system is created in the present work.

All the three constituent binary systems Mg–Zn, Ca–Zn and Mg–Ca and the ternary Mg–Ca–Zn system itself have been optimized previously. However, the two constituent binary systems Mg–Zn and Ca–Zn and the ternary Mg–Ca–Zn system have been re-optimized in the present work for the following reasons: (a) the Laves C14 phase in the Mg–Zn binary system is modeled using the compound energy formalism (CEF) [2] and compared with the experimental data for the first time. (b) According to Terpilowski [3] the maximum short-range order (SRO) in the liquid phase occurs

near the composition of MgZn₂ Laves phase at around 60 at.% Zn in the Mg–Zn system and Hafner et al. [4] mentioned that, the Ca–Zn system belongs to the class of glass-forming binary metallic systems which also indicates the tendency for short-range ordering in the liquid phase [5]. In the present assessment, this is taken into account through the use of the Modified Quasichemical Model (MQM) [6–8] for the liquid phase. This provides better representation of the partial properties of the solutes in the Mg-rich alloys and better estimations of the properties of the ternary and higher order liquid phases [9]. (c) Two ternary compounds reported by Clark [10] were considered during modeling of the Mg–Ca–Zn ternary system after careful assessment of the different contradicting experimental results from the literature regarding the number of ternary compound formation.

The optimized Gibbs energy parameters of the third binary, Mg–Ca system, are taken from Aljarrah and Medraj [11] who also used the Modified Quasichemical Model for the liquid phase. Since they [11] modeled the Mg₂Ca Laves C14 phase as a stoichiometric compound, it is remodeled in the present work using the compound energy formalism. Thereby permitting its incorporation with the MgZn₂ phase having the same crystal structure and eventually allowing to describe both phases with a single Gibbs energy function. Three ternary interaction terms were used in order to be consistent with the available experimental data from the literature. These interaction terms do not influence the constituent binaries and were kept as small numerically as possible as

* Corresponding author. Tel.: +1 514 848 2424x3146; fax: +1 514 848 3175.

E-mail address: mmedraj@encs.concordia.ca (M. Medraj).URL: <http://www.me.concordia.ca/~emmedraj>

suggested by Chartrand and Pelton [12]. All the thermodynamic optimization and calculation have been performed in the current work using FactSage 5.5 software [13].

2. Critical evaluation of the available experimental data

The initial step of thermodynamic modeling and optimization according to CALPHAD method [14] is to collect and classify experimental data relevant to Gibbs energy as input. Crystallographic information is also useful for modeling the Gibbs energy especially for the ordered phases. The list of crystallographic information for all the phases considered in the present study is given in Table 1. The next step is to critically evaluate the already collected experimental data by identifying the inconsistent and contradicting data and choosing the most reliable sets to be used for optimization [15].

2.1. Mg–Zn binary system

2.1.1. Phase diagram

Boudouard [16] firstly determined the liquidus curve for the whole composition range by thermal analysis. But due to contamination problem, his reported experimental data will not be used in this work. Later on, the liquidus line of the Mg–Zn binary system was evaluated by Grube [17], Bruni et al. [18], Bruni and Sandonnini [19], Chadwick [20] using thermal analysis and their reported values agree reasonably well with each other. Grube [17] at first reported the intermediate phase $MgZn_2$ with a melting point of 868 K and this was confirmed by later investigators [18–20] but at a slightly lower melting point. A new compound $MgZn_5$ discovered by Chadwick [20] was later replaced by Mg_2Zn_{11} based on the more reliable X-ray diffraction analysis of Samson [21]. Afterward, Hume-Rothery and Rounsefell [22] studied the system in the composition range of 30–100 at.% Zn using thermal and microscopic analyses and their data agree fairly well with those of [17] and [20]. They

[22] also reported another new compound $MgZn$ which was later substituted with a compound having 12:13 stoichiometric ratio by Clark and Rhines [23] using X-ray diffraction analysis. Takei [24] at first discovered the compound Mg_2Zn_3 which occurs by a peritectic reaction at 683 ± 10 K where the values of Anderko et al. [25] and Park and Wyman [26] were 483 ± 5 K and 489 ± 1 K, respectively, using the same methods: thermal analysis, microscopic examination and X-ray diffraction (XRD). Takei [24] also assumed that the Mg_2Zn_3 phase is in equilibrium with the Mg terminal solid solution at room temperature which was later proved to be wrong by [23] according to whom, $MgZn$, instead of Mg_2Zn_3 , is in equilibrium with Mg terminal solid solution below 598 K and their result was confirmed by other investigators [25,26]. Contradicting results regarding the peritectic formation of the Mg_7Zn_3 compound, which was discovered by Takei [24], were found in the literature. Later on, Higashi et al. [27] resolved this issue by placing the compound on the hypo-eutectic side of the Mg-rich eutectic after careful crystal structure determination using X-ray diffraction analysis. The new composition of $Mg_{51}Zn_{20}$ (28.169 at.% Zn) differs a little from that of Mg_7Zn_3 (30 at.% Zn) suggested by previous authors and its eutectoid decomposition was confirmed by Clark and Rhines [23] which occurred at 598 K. This new composition will be used in the present work.

The solid solubility of Zn in Mg was first measured by Chadwick [20] using microscopic examination of the quenched samples; but his results seem to show too high zinc content due to the presence of silicon as impurity and will not be considered in this work. Afterward, the Mg solvus curve was reported by several investigators such as Schmidt and Hansen [28] using metallography, Grube and Burkhardt [29] using electrical resistance measurements, Schmid and Seliger [30] using X-ray diffraction and Park and Wyman [26] using X-ray diffraction and microscopic examination and their values agree fairly well with each other. Besides Park and Wyman [26] measured the Mg solidus curve according to whom the maximum solubility of Zn in Mg is 2.5 at.% Zn at 613 ± 1 K. The limited solubility of Mg in Zn was determined by Hume-Rothery and Rounsefell [22] applying metallographic analysis. They reported that the maximum solubility of Mg in Zn is 0.3 at.% Mg at 637 K. The narrow homogeneity range for the intermediate solid solution $MgZn_2$ was firstly measured by Park and Wyman [26] as 1.0 at.% Zn,

Table 1
Crystallographic information for all the solid phases considered in the Mg–Ca–Zn ternary system.

Phase	Structure type	Pearson symbol	Space group	Model ^a	Note	Reference
HCP	A3	<i>hP2</i>	<i>P6₃/mmc</i>	RM	Mg, Zn have stable HCP phase	[76]
FCC	A1	<i>cF4</i>	<i>Fm$\bar{3}m$</i>	RM	Ca has stable FCC phase	[76]
BCC	A2	<i>cI2</i>	<i>Im$\bar{3}m$</i>	RM	Ca has stable BCC phase	[76]
Laves-C14	C14	<i>hP12</i>	<i>P6₃/mmc</i>	CEF	$MgZn_2$, Mg_2Ca are stable phases	[77]
$Mg_{51}Zn_{20}$	<i>D7_b</i>	<i>oI142</i>	<i>Immm</i>	ST		[27]
$Mg_{12}Zn_{13}$				ST		[25]
Mg_2Zn_3		<i>mc110</i>	<i>B2/m</i>	ST		[23]
Mg_2Zn_{11}	<i>D8_c</i>	<i>cP39</i>	<i>Pm$\bar{3}$</i>	ST		[21]
Ca_3Zn	<i>E1_a</i>	<i>oC16</i>	<i>Cmcm</i>	ST		[48]
Ca_5Zn_3	<i>D8₁</i>	<i>tI32</i>	<i>I4/mcm</i>	ST		[47]
$CaZn$	<i>B_f</i>	<i>oC8</i>	<i>Cmcm</i>	ST		[48]
$CaZn_2$		<i>oI12</i>	<i>Imma</i>	ST		[65]
$CaZn_3$		<i>hP32</i>	<i>P6₃/mmc</i>	ST		[48]
$CaZn_5$	<i>D2_d</i>	<i>hP6</i>	<i>P6₃/mmm</i>	ST		[66]
$CaZn_{11}$		<i>tI48</i>	<i>I4₁/amd</i>	ST		[67]
$CaZn_{13}$	<i>D2₃</i>	<i>cF112</i>	<i>Fm$\bar{3}c$</i>	ST		[68]
$Ca_2Mg_6Zn_3$		<i>hP22</i>	<i>P$\bar{3}1c$</i>	ST		[56]
$Ca_2Mg_5Zn_{13}$				ST	No information available	

^a RM = random mixing, CEF = compound energy formalism, ST = stoichiometric compound.

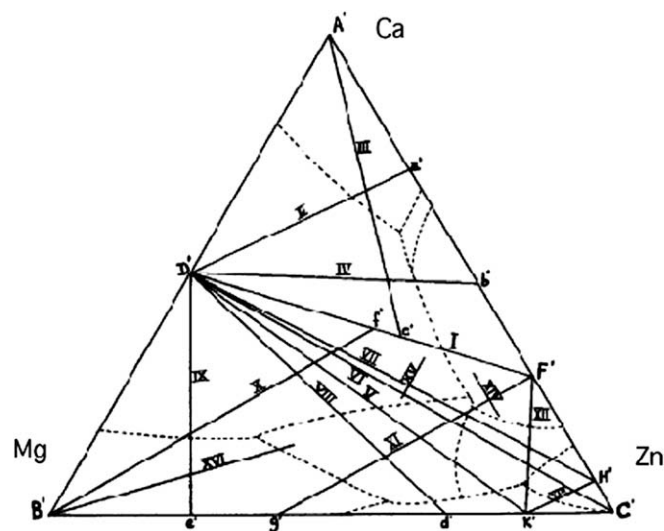


Fig. 1. The liquidus projection of the Mg–Ca–Zn ternary system, as drawn by Paris [45], indicating the locations of his sixteen isopleths. The axes are in mass fraction.

Table 2
Optimized model parameters of the liquid binary Mg–Zn, Ca–Zn and Mg–Ca phases.

Atom–atom “coordination numbers” ^a				Gibbs energies of pair exchange reactions (J/mol)
A	B	Z _{AB} ^A	Z _{BA} ^B	
Mg	Zn	6	4	$\Delta^{\text{ex}}G_{\text{MgZn}}^{\text{liq}} = -8100.84 + 2.26T + (-146.3 - 3.55T)X_{\text{MgMg}} + (-79.42 - 4.24T)X_{\text{ZnZn}}$
Ca	Zn	6	3	$\Delta^{\text{ex}}G_{\text{CaZn}}^{\text{liq}} = -17765 + 0.084T - 10282.8X_{\text{CaCa}} - 7942.0X_{\text{ZnZn}}$
Mg	Ca	5	4	$\Delta^{\text{ex}}G_{\text{MgCa}}^{\text{liq}} = -13187.9 + 7.98T + (6908.55 - 23.0T)X_{\text{CaCa}} + (8899.22 - 15.93T)X_{\text{MgMg}}$ ^b

^a For all pure elements (A = Mg, Ca and Zn), Z_{AA}^A = 6.

^b Parameter was taken from Aljarrah and Medraj [11].

from 66 at.% Zn at 689 K to 67.1 at.% Zn at 654 K and their reported values will be compared with the current findings.

An assessment of the Mg–Zn system was performed by Clark et al. [31] based on the experimental work of Chadwick [20], Hume-Rothery and Rounsefell [22] and Park and Wyman [26]. On the other hand, Agarwal et al. [32] and Liang et al. [33] optimized the system where both of them used Redlich–Kister polynomial [34] for the liquid phase which cannot account for the presence of short-range ordering (SRO) in the liquid phase. Hence this feature will be handled in the present work using the Modified Quasichemical Model.

2.1.2. Thermodynamic properties

Pyka [35] and Agarwal and Sommer [36] measured the enthalpy of mixing of the Mg–Zn liquid using calorimetric measurement at different temperatures where the values of [35] showed

temperature independence but the values of [36] at 933 K showed some deviation from the other values in the Mg-rich side. This is perhaps due to the stabilization of one or more Mg-rich intermediate phases and it is an indication of short-range ordering in the liquid phase as suggested by [36]. Terpilowski [3], Chiotti and Stevens [37], Moser [38] and Pogodaev and Lukashenko [39] measured the activity of Mg over Mg–Zn liquid at different temperatures using electromotive force (EMF) technique. On the other hand, the activity of Zn in the liquid alloy was calculated by Terpilowski [3] using Gibbs–Duhem equation at 923 K. The same property was experimentally measured by Pogodaev and Lukashenko [39] at 1073 K and Kozuka et al. [40] at 943 K where both of them used vapor pressure measurement. Terpilowski [3] also measured the partial enthalpy of Mg at 923 K whereas the same property was measured by Agarwal et al. [32] at 873 K using calorimetric method and their results will be compared with the values of [3] and those from the present work.

Table 3
Comparison between calculated and experimental invariant points in the Mg–Zn system.

Reaction type	Reaction	Composition (at.% Zn)	Temperature (K)	Reference
Eutectic	L ↔ Mg ₅₁ Zn ₂₀ + Mg ₁₂ Zn ₁₃	28.9	614.0	This work
		–	617.0	[17]
		28.7	613.0	[19]
		30.2	615.5	[20]
		28.1	613.0 ± 1.0	[26]
		30.0	616.0 ± 1.0	[25]
	L ↔ Mg ₂ Zn ₁₁ + Zn.Hcp	92.9	640.0	This work
		–	641.0	[17]
		92.5	636.0	[18]
		–	641.0	[20]
		92.2	637.0	[22]
		92.2	637.0	[26]
Peritectic	L + Mg.Hcp ↔ Mg ₅₁ Zn ₂₀	28.9	614.0	This work
		28.3	615.0 ± 1.0	[26]
		–	617.0–621.0	[25]
	L + Mg ₂ Zn ₃ ↔ Mg ₁₂ Zn ₁₃	29.7	620.0	This work
		–	627.0	[22]
		29.0	620.0 ± 1.0	[26]
		–	622.0 ± 2.0	[25]
	L + Laves.C14 ↔ Mg ₂ Zn ₃	37.1	689.0	This work
		–	683.0 ± 10.0	[24]
		–	689.0 ± 1.0	[26]
		–	683.0 ± 1.0	[25]
	L + Laves.C14 ↔ Mg ₂ Zn ₁₁	90.0	654.0	This work
–		654.0	[26]	
–		653.5	[22]	
–		653.5	[22]	
Congruent	L ↔ Laves.C14	66.7	862.0	This work
		66.7	868.0	[17]
		66.7	862.0	[19]
		66.7	858.0	[20]
		66.7	863.0	[22]
		66.7	861.0	[26]
Eutectoid	Mg ₅₁ Zn ₂₀ ↔ Mg.Hcp + Mg ₁₂ Zn ₁₃	28.1	599.0	This work
		–	598.0	[23]

Table 4
Optimized model parameters of all the terminal solid solutions and stoichiometric compounds of Mg–Zn, Ca–Zn and Mg–Ca systems.

Terminal solid solution			
Phase	Gibbs energy parameters (J/mol)		
Mg_Hcp, Zn_Hcp	$G_{\text{Mg,Zn}}^{\text{Hcp}} = -2090.19 + 5.21T$		
Mg_Hcp	$G_{\text{Mg,Ca}}^{\text{Hcp}} = 1710.06 + (-12.32T)$		
Stoichiometric compounds			
Compound	$\Delta H_{298.15\text{K}}^0$ (J/mol-atom)	$\Delta S_{298.15\text{K}}^0$ (J/mol-atom K)	C _p (J/mol K)
Mg ₅₁ Zn ₂₀	–5276.06	–0.54	$C_p = 51 \times C_p(\text{Mg, Hcp-A3}) + 20 \times C_p(\text{Zn, Hcp-Zn})$
Mg ₁₂ Zn ₁₃	–10440.03	–2.35	$C_p = 12 \times C_p(\text{Mg, Hcp-A3}) + 13 \times C_p(\text{Zn, Hcp-Zn})$
Mg ₂ Zn ₃	–10877.24	–0.92	$C_p = 2 \times C_p(\text{Mg, Hcp-A3}) + 3 \times C_p(\text{Zn, Hcp-Zn})$
Mg ₂ Zn ₁₁	–9882.95	–6.85	$C_p = 2 \times C_p(\text{Mg, Hcp-A3}) + 11 \times C_p(\text{Zn, Hcp-Zn})$
Ca ₃ Zn	–11906.31	–3.82	$C_p = 3 \times C_p(\text{Ca, Bcc-A2}) + C_p(\text{Zn, Hcp-Zn})$
Ca ₅ Zn ₃	–14486.92	–0.88	$C_p = 5 \times C_p(\text{Ca, Bcc-A2}) + 3 \times C_p(\text{Zn, Hcp-Zn})$
CaZn	–17842.54	–0.53	$C_p = C_p(\text{Ca, Bcc-A2}) + C_p(\text{Zn, Hcp-Zn})$
CaZn ₂	–22728.35	–1.48	$C_p = C_p(\text{Ca, Bcc-A2}) + 2 \times C_p(\text{Zn, Hcp-Zn})$
CaZn ₃	–21418.76	–2.66	$C_p = C_p(\text{Ca, Bcc-A2}) + 3 \times C_p(\text{Zn, Hcp-Zn})$
CaZn ₅	–19997.51	–3.84	$C_p = C_p(\text{Ca, Bcc-A2}) + 5 \times C_p(\text{Zn, Hcp-Zn})$
CaZn ₁₁	–14798.75	–3.62	$C_p = C_p(\text{Ca, Bcc-A2}) + 11 \times C_p(\text{Zn, Hcp-Zn})$
CaZn ₁₃	–14149.64	–4.23	$C_p = C_p(\text{Ca, Bcc-A2}) + 13 \times C_p(\text{Zn, Hcp-Zn})$

Table 5
Optimized model parameters for ternary solutions and compounds in the present study.

Laves-C14 (MgZn ₂ -type): (Mg,Ca,Zn) ₂ (Mg,Ca,Zn) (J/mol)			
${}^0G_{\text{Mg:Mg}} = 3G(\text{Mg, Hcp-A3}) + 11653.84$			
${}^0G_{\text{Ca:Ca}} = 3G(\text{Ca, Bcc-A2}) + 126236.0$			
${}^0G_{\text{Zn:Zn}} = 3G(\text{Zn, Hcp-Zn}) + 22521.84$			
${}^0G_{\text{Mg:Zn}} = G(\text{Mg, Hcp-A3}) + 2G(\text{Zn, Hcp-Zn}) - 34296.9 + 1.7137$			${}^0G_{\text{Zn:Mg}} = 2G(\text{Mg, Hcp-A3}) + G(\text{Zn, Hcp-Zn}) + 56973.4$
${}^0G_{\text{Mg:Ca}} = 2G(\text{Mg, Hcp-A3}) + G(\text{Ca, Bcc-A2}) - 33440.0 + 8.367$			${}^0G_{\text{Ca:Mg}} = G(\text{Mg, Hcp-A3}) + 2G(\text{Ca, Bcc-A2}) + 16720.0$
${}^0G_{\text{Ca:Zn}} = G(\text{Ca, Bcc-A2}) + 2G(\text{Zn, Hcp-Zn}) + 71060.0$			${}^0G_{\text{Zn:Ca}} = 2G(\text{Ca, Bcc-A2}) + G(\text{Zn, Hcp-Zn}) + 16720.0$
${}^0L_{\text{Mg,Zn:Mg}} = {}^0L_{\text{Mg,Zn:Zn}} = 33866.55$			
${}^0L_{\text{Mg:Mg,Zn}} = {}^0L_{\text{Zn:Mg,Zn}} = 4.20$			
${}^0L_{\text{Mg,Ca}} = {}^0L_{\text{Mg,Ca}} = {}^0L_{\text{Mg,Mg,Ca}} = {}^0L_{\text{Ca,Mg,Ca}} = 42019.28$			
Liquid phase (J/mol)			
$L_{\text{MgCa(Zn)}} = -12,540$, $L_{\text{MgZn(Ca)}} = -12,540$, $L_{\text{CaZn(Mg)}} = 4180$			
Stoichiometric compounds			
Compound	$\Delta H_{298.15\text{ K}}^0$ (J/mol-atom)	$\Delta S_{298.15\text{ K}}^0$ (J/mol-atom K)	C_p (J/mol K)
$\text{Ca}_2\text{Mg}_6\text{Zn}_3$	-14801.83	-0.17	$C_p = 2 \times C_p(\text{Ca,Bcc-A2}) + 6 \times C_p(\text{Mg,Hcp-A3}) + 3 \times C_p(\text{Zn,Hcp-Zn})$
$\text{Ca}_2\text{Mg}_5\text{Zn}_{13}$	-16740.51	-0.10	$C_p = 2 \times C_p(\text{Ca,Bcc-A2}) + 5 \times C_p(\text{Mg,Hcp-A3}) + 13 \times C_p(\text{Zn,Hcp-Zn})$

The enthalpy of formation of the three intermediate compounds Mg₁₂Zn₁₃, MgZn₂ and Mg₂Zn₁₁ was determined by Schneider et al. [41] using reaction calorimetry, where the same property for the first two phases was measured by King and Kleppa [42] using tin solution calorimetry and for all the phases by Pedokand et al. [43] using EMF measurement. All these experimental data will be considered during the present study.

2.2. Ca–Zn binary system

2.2.1. Phase diagram

Very limited amounts of experimental data have been found in the literature for the Ca–Zn system. The earlier works of Donski [44] and Paris [45] will be abandoned in the present work due to contamination problem during sample preparation. Liquidus data of Messing et al. [46] suggested to be most reliable in terms of sample preparation and experimental methods. They performed differential thermal analysis (DTA) supplemented by X-ray diffraction analysis (XRD) to investigate the liquidus line. Because of the high vapor pressure of the Ca–Zn alloys above 50 at.% Zn, Messing et al. [46] also used vapor effusion measurement for compound identification. They reported accuracy of ± 5 K and predicted eight intermediate stoichiometric compounds: Ca₃Zn, Ca₇Zn₄, CaZn, CaZn₂, Ca₇Zn₂₀, CaZn₅, CaZn₁₁ and CaZn₁₃. Apart from CaZn₂, CaZn₅ and CaZn₁₁, all compounds undergo peritectic decomposition. Later on, the compounds Ca₇Zn₄ and Ca₇Zn₂₀ designated by [46] were replaced with Ca₅Zn₃ and CaZn₃, respectively, based on the more accurate crystallographic investigations of Bruzzone et al. [47] and Fornasini and Merlo [48] and these will be used in the present optimization.

2.2.2. Thermodynamic properties

Itkin and Alcock [49] evaluated the activity of Zn at 1073 K during their assessment from the vapor pressure measurement data of Chiotti and Hecht [50] who used dewpoint method for samples containing greater than 50 at.% Zn and the Knudsen effusion method for lower Zn concentration. Delcet and Egan [51] determined the activity of Ca at 1073 K using EMF measurement. No experimental data for the enthalpy of mixing of the liquid phase could be found in the literature. The enthalpy of formation for all the intermediate phases was calculated by Chiotti and Hecht [50]

from the temperature dependence of the experimental Zn vapor pressure data and phase equilibrium condition.

2.3. Mg–Ca–Zn ternary system

The experimental work on the liquidus curve of the Mg–Ca–Zn ternary system was first carried out by Paris [45] by cooling of 189 different alloys in sixteen different isopleths as shown in Fig. 1. Although Paris' [45] samples might have had contamination problem, as mentioned earlier, they were used during the optimization of the ternary Mg–Ca–Zn system because not many other experimental works on this ternary system could be found in the literature. Based on his thermal analysis and metallography, Paris reported one ternary compound with a composition of Ca₂Mg₅Zn₅ but did not provide any crystallographic information for it. The isothermal section in the Mg–Zn side of the Mg–Ca–Zn system at 608 K was studied by Clark [10] using metallography and powder X-ray diffraction on seventy-six alloys searching for other ternary phases. This was performed using the diffusion couple method and two ternary compounds were reported, namely β and ω which were stable at room temperature under equilibrium condition and disputed the composition of Ca₂Mg₅Zn₅ reported by Paris [45]. The compositions of the two ternary compounds were mentioned by Clark later on in the Joint Committee on Powder Diffraction Standards (JCPDS) [52,53] which were Ca₂Mg₆Zn₃ for β and Ca₂Mg₅Zn₁₃ for ω . No liquid phase was detected at 608 K during his experiment. Then recently, Larinova et al. [54] worked on this system using XRD and Jardim et al. [55,56] using XRD, transmission electron microscopy (TEM), energy dispersive X-ray spectroscopy (EDS) coupled with scanning transmission electron microscopy (STEM) and scanning electron microscopy (SEM). Both of them reported a ternary compound and determined with Ca₂Mg₆Zn₃ composition which is similar to the first compound given in the JCPDS card reported by Clark [10]. Larinova et al. [54] and Jardim et al. [55,56] prepared their samples in the form of ribbons using melt spinning technique and heat treated those samples for almost 1 h at 673 K and 473 K, respectively. Jardim et al. [56] also reported the crystallographic information of the compound Ca₂Mg₆Zn₃.

A computational thermodynamic model on this system was reported by Brubaker and Liu [57] where they considered only the first ternary compound, reported by Clark [10]. Their proposed model was based on the random mixing of atoms in the liquid

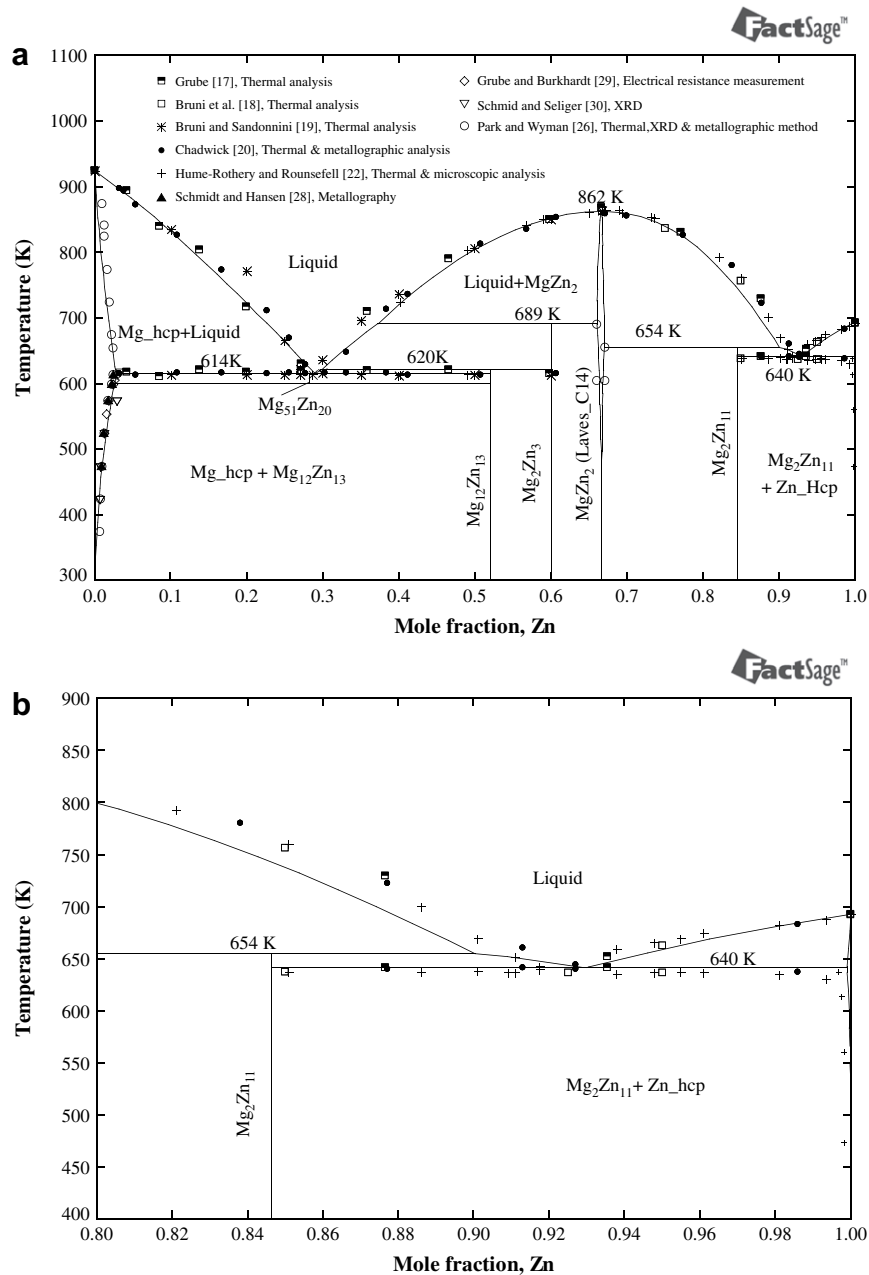


Fig. 2. (a) Re-optimized Mg–Zn phase diagram, (b) Zn-rich portion of the Mg–Zn system compared with experimental data.

phase, which cannot properly handle the presence of short-range ordering. For these reasons, this system is being remodeled using the modified quasichemical model in this work.

3. Analytical description of the employed thermodynamic models

The Gibbs energy of pure element i ($i = \text{Mg, Ca and Zn}$) in a certain phase ϕ is described as a function of temperature by the following equation:

$${}^0G_i^\phi(T) = a + bT + cT \ln T + dT^2 + eT^3 + fT^{-1} + gT^7 + hT^{-9} \quad (1)$$

where ${}^0G_i^\phi(T)$ is the Gibbs energy at standard state and T is the absolute temperature. The value of the coefficients a to h are taken

from the SGTE (Scientific Group Thermodata Europe) compilation by Dinsdale [58].

The Gibbs energy for stoichiometric compounds is described by the following equation:

$$G^\phi = x_i {}^0G_i^{\phi_1} + x_j {}^0G_j^{\phi_2} + \Delta G_f \quad (2)$$

where ϕ denotes the phase of interest, x_i and x_j are the mole fraction of components i and j and ${}^0G_i^{\phi_1}$, ${}^0G_j^{\phi_2}$ represent the Gibbs energy in their standard state and $\Delta G_f = a + bT$ is the Gibbs energy of formation per mole of atoms of the stoichiometric compound where the parameters a and b are obtained by optimization using experimental results of phase equilibria and thermodynamic data.

Random solution model was used to describe the disorder terminal solid solution phases which can be expressed as:

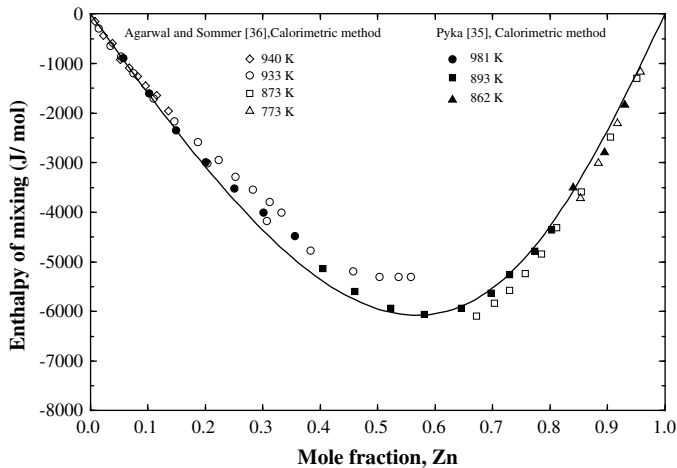


Fig. 3. Calculated enthalpies of mixing of Mg and Zn in liquid Mg–Zn alloy at 981 K in comparison with the experimental results.

$$G = x_i^0 G_i^\phi + x_j^0 G_j^\phi + RT [x_i \ln x_i + x_j \ln x_j] + {}^{ex}G^\phi \quad (3)$$

The excess Gibbs energy ${}^{ex}G^\phi$ is expressed using the Redlich–Kister polynomial model [34] as follows:

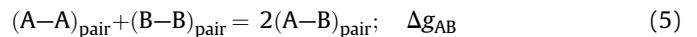
$${}^{ex}G^\phi = x_i \cdot x_j \sum_{n=0}^{m} {}^n L_{ij}^\phi (x_i - x_j)^n \text{ with } {}^n L_{ij}^\phi = a_n + b_n \times T \quad (n = 0, 1 \dots m) \quad (4)$$

where ${}^n L_{ij}^\phi$ is the interaction parameters, $m + 1$ is the number of terms, a_n and b_n are the parameters of the model that need to be optimized considering the experimental phase diagram and thermodynamic data.

In the present work, two terminal solid solution phases Mg₂Hcp and Zn₂Hcp of the Mg–Zn system were modeled using one set Gibbs energy description.

The Modified Quasichemical Model (MQM) in the pair approximation was selected to describe the liquid phases of the constituent binary systems. Alloy systems which show a strong compound forming tendency in the solid state (i.e. Ca–Zn, Mg–Zn, etc.) also

display a pronounced minimum in the enthalpy of mixing of the liquid phase and this is caused due to the existence of short-range ordering [59]. The Bragg–Williams (BW) random-mixing model is not able to represent the binary solutions with short-range ordering (SRO) and to describe the enthalpy and entropy of mixing functions properly. The “associate” or “molecular” model [60] was also proposed to deal with the short-range ordering. However associate model assumes that some molecules occupy some of the atomic sites which are not physically sound. Another important weakness of the “associate” model is its inability to predict the correct thermodynamic properties of ternary solutions when the binary sub-systems exhibit short-range ordering [61]. The MQM has been described extensively elsewhere [6–8] and will be outlined briefly here. In the pair approximation of the MQM, the simple pair exchange reaction between atoms A and B on neighboring lattice sites is considered as follows:



where $(A-B)$ represents a first-nearest neighbor pair and Δg_{AB} is the nonconfigurational Gibbs energy change for the formation of two moles of $(A-B)$ pairs. According to Pelton et al. [6–8] the molar Gibbs energy of a binary A–B solution is given as:

$$G^{\text{liq}} = (n_A^0 g_A^{\text{liq}} + n_B^0 g_B^{\text{liq}}) - T \Delta S^{\text{config}} + \left(\frac{n_{AB}}{2}\right) \Delta g_{AB} \quad (6)$$

Here n_A and n_B are number of moles of components A and B, n_{AB} is the number of moles of $(A-B)$ pairs, ΔS^{config} is the configurational entropy of mixing given by random distribution of the $(A-A)$, $(B-B)$ and $(A-B)$ pairs.

Pelton et al. [6] made modification to equation (6) by expanding Δg_{AB} as a polynomial in terms of the pair fraction X_{AA} and X_{BB} as shown in equation (7)

$$\Delta g_{AB} = \Delta g_{AB}^0 + \sum_{i \geq 1} g_{AB}^{i0} X_{AA}^i + \sum_{j \geq 1} g_{AB}^{0j} X_{BB}^j \quad (7)$$

where Δg_{AB}^0 , g_{AB}^{i0} and g_{AB}^{0j} are the model parameters to be optimized and can be expressed as functions of temperature ($\Delta g_{AB}^0 = a + bT$). In addition, further modification has been made in the coordination numbers by making them composition-dependent in order to overcome the drawbacks of the constant coordination numbers. This modification can be expressed as:

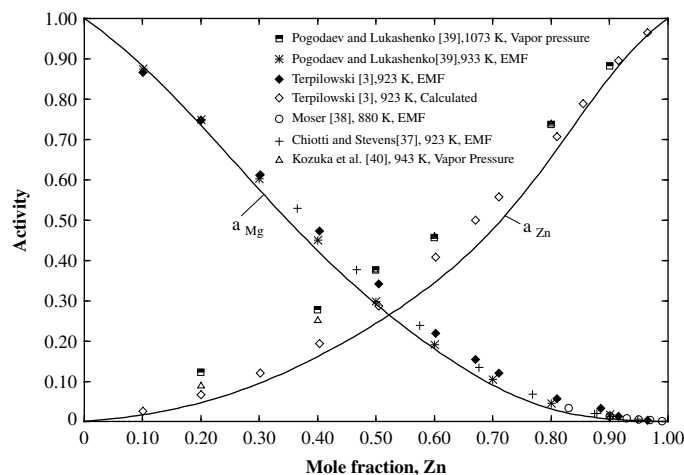


Fig. 4. Calculated activities of Mg and Zn (relative to pure liquid Mg and Zn) in Mg–Zn alloys at 923 K and 1073 K, respectively.

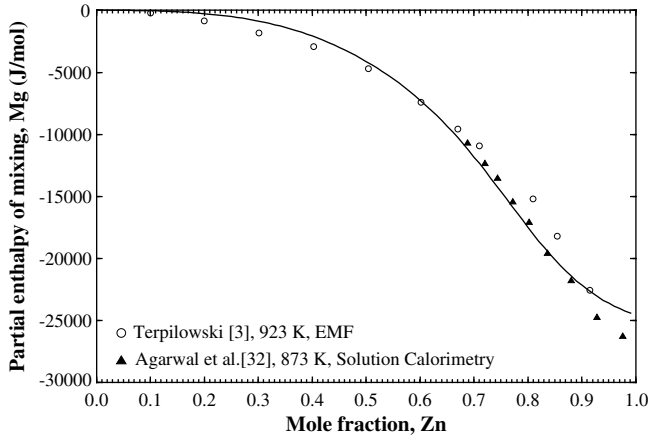


Fig. 5. Calculated partial enthalpy of mixing for Mg in the Mg–Zn liquid at 923 K.

$$\frac{1}{Z_A} = \frac{1}{Z_{AA}^A} \left(\frac{2n_{AA}}{2n_{AA} + n_{AB}} \right) + \frac{1}{Z_{AB}^A} \left(\frac{n_{AB}}{2n_{AA} + n_{AB}} \right) \quad (8)$$

$$\frac{1}{Z_B} = \frac{1}{Z_{BB}^B} \left(\frac{2n_{BB}}{2n_{BB} + n_{AB}} \right) + \frac{1}{Z_{BA}^B} \left(\frac{n_{AB}}{2n_{BB} + n_{AB}} \right) \quad (9)$$

where Z_{AA}^A and Z_{AB}^A are the values of Z_A when all nearest neighbors of an A atom are As, and when all nearest neighbors of A atom are Bs, respectively. Similarly for Z_{BB}^B and Z_{BA}^B . The composition of maximum short-range ordering is determined by the ratio Z_{BA}^B/Z_{AB}^A . Values of Z_{AB}^A and Z_{BA}^B are unique to the A–B binary system and should be carefully determined to fit the thermodynamic experimental data (enthalpy of mixing, activity, etc.). The values of Z_{AA}^A and Z_{BB}^B are common for all systems containing A and B as components. The coordination number of the pure elements in the metallic solution, $Z_{MgMg}^{Mg} = Z_{CaCa}^{Ca} = Z_{ZnZn}^{Zn}$, was set to be 6. Because this value gave the best possible fit for many binary systems and was also recommended by Pelton et al. [6–8]. The values of Z_{MgZn}^{Mg} , Z_{ZnMg}^{Zn} , Z_{CaZn}^{Ca} , Z_{ZnCa}^{Zn} , Z_{MgCa}^{Mg} and Z_{CaMg}^{Ca} are chosen to permit the composition of maximum short-range ordering in the binary system to be consistent with the composition that corresponds to the minimum enthalpy of mixing and are listed in Table 2. In order to set the composition of maximum SRO at 60 at.% Mg as suggested by [3] in the Mg–Zn system, we set $Z_{MgZn}^{Mg} = 6$ and $Z_{ZnMg}^{Zn} = 4$. For the Ca–Zn system, the maximum short-range ordering near 66 at.% Zn was obtained by setting $Z_{CaZn}^{Ca} = 6$ and $Z_{ZnCa}^{Zn} = 3$. Aljarrah and Medraj [11] set the values as $Z_{MgCa}^{Mg} = 5$ and $Z_{CaMg}^{Ca} = 4$ in order to set the composition of maximum SRO near the composition 55 at.% Mg in the Mg–Ca system.

The Gibbs energy of the ordered intermediate solution phase is described by the compound energy formalism (CEF) [2] which can be expressed as:

$$G = G^{\text{ref}} + G^{\text{ideal}} + G^{\text{excess}} \quad (10)$$

$$G^{\text{ref}} = \sum y_i^l y_j^m \dots y_k^q G_{(ij:\dots:k)}^0 \quad (11)$$

$$G^{\text{ideal}} = RT \sum_l f_l \sum_i y_i^l \ln y_i^l \quad (12)$$

$$G^{\text{excess}} = \sum y_i^l y_j^m y_k^q \sum_{\gamma=0}^{\gamma} \gamma L_{(ij):k} \times (y_i^l - y_j^m)^\gamma \quad (13)$$

where ij, \dots, k represent components or vacancy, l, m and q represent sublattices. y_i^l is the site fraction of component i on sublattice l . f_l is the fraction of sublattice l relative to the total lattice sites. $G_{(ij:\dots:k)}^0$ represents the energy of a real or hypothetical compound (end member). $\gamma L_{(ij):k}$ represents the interaction parameters between components i and j on one sublattice when the other sublattice is occupied only by k .

The Laves phases observed in the Mg–Zn and Mg–Ca systems are $MgZn_2$ and Mg_2Ca , have the same crystal structure and CEF is employed to model them using one set of Gibbs energy parameters. Modeling of these phases requires information regarding the crystal structure and homogeneity range. In the present work, these two phases have been modeled in a way so that all the three components occupy both sublattices as $(Mg,Ca,Zn)_2(Mg,Ca,Zn)_1$. This model of two sublattices covers the whole composition range and therefore the homogeneity range of $0.66 \leq x_{Zn} \leq 0.671$ which was reported by [26] could be obtained from this model for $MgZn_2$ phase. $MgZn_2$ and Mg_2Ca are stable phases in their corresponding binaries, hence $G_{Mg:Zn}^0$ and $G_{Mg:Ca}^0$ are set equal to the actual Gibbs energies of the phases. The Gibbs energies of the other hypothetical end members are arbitrarily set to high positive values. Although $CaZn_2$ is a stable phase in the Mg–Ca–Zn ternary system, it is not a Laves phase and it is modeled using stoichiometric model in the present work. The values of the interaction parameters of equation (13) are kept large positive due to the narrow homogeneity range of the $MgZn_2$ phase and the stoichiometry of the Mg_2Ca phase.

All the optimized model parameters of different phases in the Mg–Ca–Zn ternary system are summarized in Tables 2, 4 and 5.

4. Results and discussions

4.1. Mg–Zn binary system

4.1.1. Phase diagram

The calculated Mg–Zn binary system is shown in Fig. 2, which shows reasonable agreement with the experimental data from the literature. From the same figure, it can be seen that there are two eutectic points, four peritectic points and all the intermediate compounds melt incongruently except $MgZn_2$. Table 3 lists all the calculated invariant points in comparison with the experimental data from the literature.

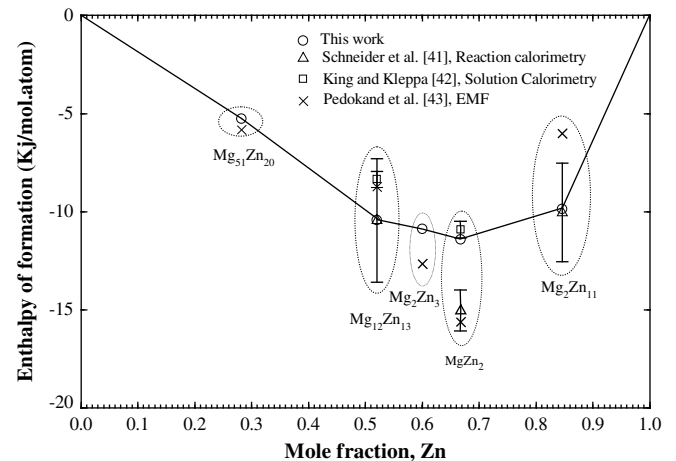


Fig. 6. Calculated enthalpies of formation at 298.15 K for the compounds in the Mg–Zn system. Reference states are Mg–Hcp and Zn–Hcp.

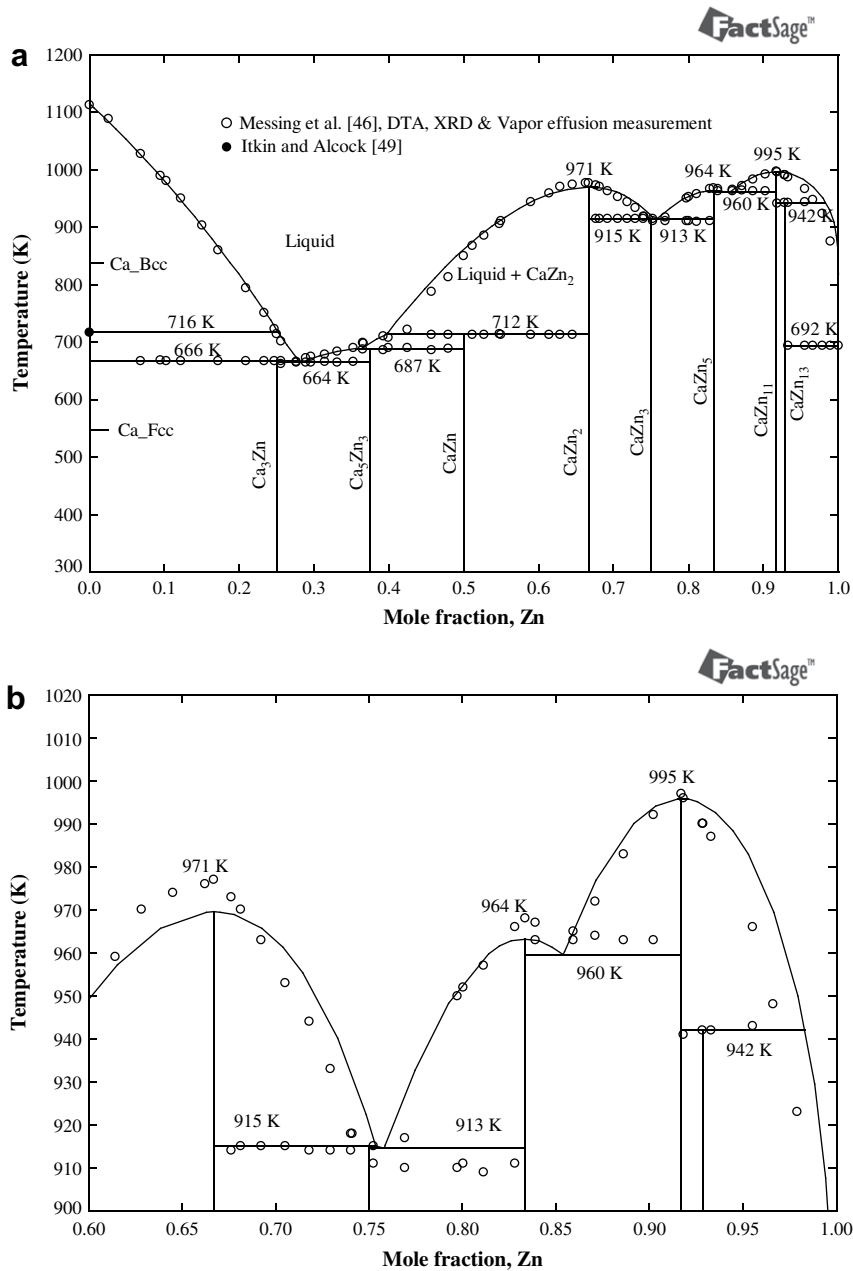


Fig. 7. (a) Re-optimized Ca–Zn phase diagram, (b) Zn-rich portion of the Ca–Zn system compared to experimental data.

The maximum solubility of Zn in Mg was found to be 2.82 at.% Zn which is close to the experimental value of 2.9 at.% Zn reported by Grube and Burkhardt [29]. However, Park and Wyman [26] and Schmidt and Hansen [28] reported this as 2.5 at.% Zn and 2.4 at.% Zn, respectively. Hence the value from the present calculation lies between the experimental values of [26,28,29]. On the other hand, a very limited solubility of Mg in Zn (0.1 at.% Mg) was observed. This is in the same order of magnitude of the experimental value of Hume-Rothery and Rounsefell [22] (0.3 at.% Mg). Moreover, it is worth noting that, both Agarwal et al. [32] and Liang et al. [33] used two Redlich–Kister terms to describe the terminal solid solution where in the present work, one Redlich–Kister term was used to model this phase. The congruent melting temperature of the intermediate compound MgZn_2 was found to be 862 K which is in good agreement with most of the experimental data except Grube [17], according to whom the value was

868 K which is the highest among all the available experimental data.

4.1.2. Thermodynamic properties

The calculated enthalpy of mixing of the Mg–Zn liquid at 981 K, shown in Fig. 3, is in good agreement with the experimental data from the literature except for the small deviation from the data of Agarwal and Sommer [36] at 933 K near the composition range 20–55 at.% Zn. Nevertheless the current results agree well with those of Pyka [35]. It is also worth noting from the same figure that, the minimum value of enthalpy of mixing occurs near 60 at.% Zn which is very close to the value suggested by Terpilowski [3], where maximum short-range ordering takes place. The calculated activities of Mg and Zn components over the liquid phase at 923 K and 1073 K are shown in Fig. 4 where the activity of Mg shows good consistency with the experimental data. Some deviation can be

Table 6

Comparison between calculated and experimental invariant points in the Ca–Zn system.

Reaction type	Reaction	Composition (at.% Zn)	Temperature (K)	Reference
Eutectic	$L \leftrightarrow Ca_3Zn + Ca_5Zn_3$	28.4	664	This work
		27.4	664	[46]
	$L \leftrightarrow CaZn_3 + CaZn_5$	76.0	913	This work
		76.4	911	[46]
	$L \leftrightarrow CaZn_5 + CaZn_{11}$	85.4	960	This work
	86.4	963	[46]	
Peritectic	$L + Ca_{Bcc} \leftrightarrow Ca_3Zn$	27.9	666	This work
		–	667	[46]
	$L + CaZn \leftrightarrow Ca_5Zn_3$	36.4	687	This work
		–	687	[46]
	$L + CaZn_2 \leftrightarrow CaZn$	39.7	712	This work
		–	712	[46]
	$L + CaZn_2 \leftrightarrow CaZn_3$	75.3	915	This work
		–	915	[46]
$L + CaZn_{11} \leftrightarrow CaZn_{13}$	98.3	942	This work	
	–	942	[46]	
Congruent	$L \leftrightarrow CaZn_2$	66.7	971	This work
		66.7	977	[46]
	$L \leftrightarrow CaZn_5$	83.3	964	This work
		83.3	968	[46]
	$L \leftrightarrow CaZn_{11}$	91.7	995	This work
		91.7	997	[46]
Allotropic	$Ca_{Fcc} \leftrightarrow Ca_{Bcc}$	0.0	716	This work
		0.0	718	[46]
		0.0	716	[49]

seen between the calculated value and the experimental data of Pogodaev and Lukashenko [39] and Kozuka et al. [40] for the activity of Zn near 40–80 at.% Zn. This discrepancy is perhaps due to the less accurate vapor pressure method used by [39,40]. However, the calculated activity curve of Zn shows reasonable agreement with the calculated results of Terpilowski [3] where he extracted the values from the activity of Mg using the Gibbs–Duhem equation. Fig. 5 shows the partial enthalpy of mixing for Mg ($\Delta\bar{H}_{Mg}$) in the Mg–Zn liquid at 923 K in comparison with the experimental results from the literature where good consistency was accomplished.

Comparison between the enthalpies of formation of the intermediate compounds and the experimental results from the literature is shown in Fig. 6. Reasonable consistency was achieved with

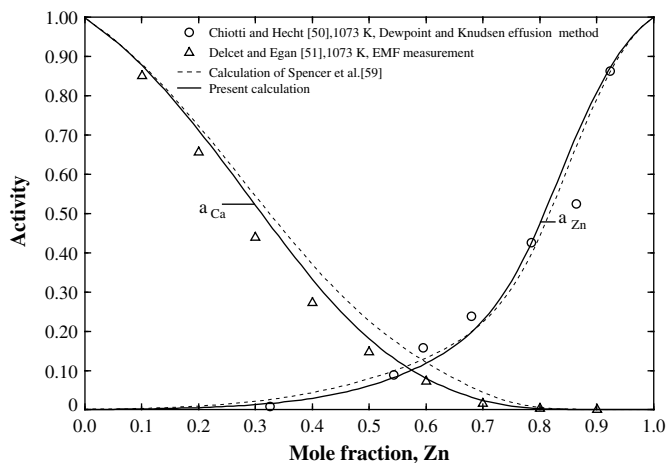


Fig. 8. Calculated activities of Ca and Zn (relative to pure liquid Ca and Zn) in Ca–Zn alloys at 1073 K.

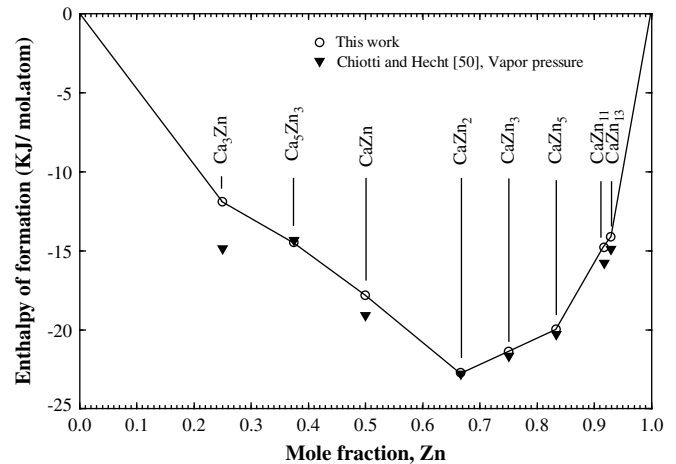


Fig. 9. Optimized enthalpies of formation at 298.15 K for the compounds in the Ca–Zn system.

the experimental values within the error limits. The enthalpy of formation for Mg_2Zn_{11} phase measured by Pedokand et al. [43] is not consistent with the experimental value of Schneider et al. [41] as well as the calculated value in this work. However, the data of Schneider et al. [41] is considered more reliable because of the use of reaction calorimetry.

4.2. Ca–Zn binary system

4.2.1. Phase diagram

Most recently Spencer et al. [59] evaluated the experimental work of the Ca–Zn system and carried out a thermodynamic calculation of this system using the Modified Quasichemical Model for the liquid phase. However their work has just appeared after this system has been modeled in this work. In addition, to build a self-consistent Mg alloy database, an independent re-optimization and thorough assessment on this system has been performed in the present work. Fig. 7 shows the optimized phase diagram of the Ca–Zn system along with the experimental results of Messing et al. [46]. The calculated phase diagram shows reasonable agreement with the experimental data from the literature. The allotropic transformation α (Fcc_A1) \leftrightarrow β (Bcc_A2) of Ca takes place at 716 K which is the same as the value adopted by Itkin and Alcock [49]

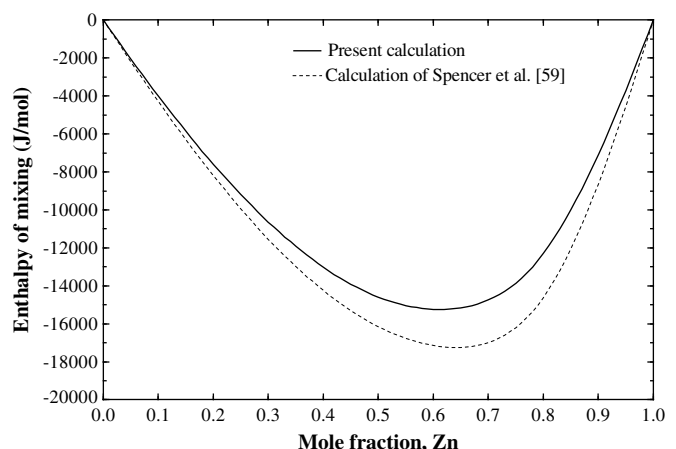


Fig. 10. Enthalpy of mixing of liquid Ca–Zn alloys at 1173 K.

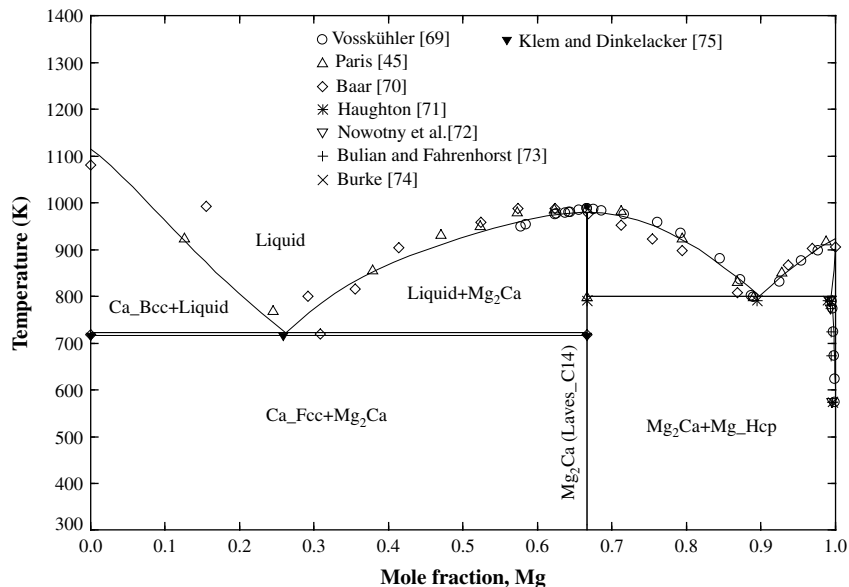


Fig. 11. [69,70,71,72,73,74,75] phase diagram of [11] including the re-optimized Mg₂Ca Laves phase from the present work.

during their assessment of this system. Previously, Brubaker and Liu [62] modeled the CaZn₃ phase as congruently melting compound but in that case the liquidus of CaZn₃ on the Ca-rich side becomes too flat and according to Okamoto and Massalski [63], this is thermodynamically improbable. Hence in the present work, incongruent melting of the CaZn₃ phase is considered which is supported by the recent work of Spencer et al. [59]. Neither Ca nor Zn displays any solubility in one another and hence were not included in the present work. The temperatures and phase composition of invariant reactions are presented in Table 6. It can be seen from the same table that the maximum difference between the experimental and calculated results is 6 K in temperature and 1.0 at.% in composition.

4.2.2. Thermodynamic properties

The calculated activities of Ca and Zn over the Ca–Zn liquid at 1073 K are shown in Fig. 8 where a reasonable agreement was accomplished between the calculated curves and the experimental points. Comparison is also made with the assessment of [59] in the same figure. Better agreement was not possible without deteriorating the liquidus curve. Fig. 9 shows a comparison between the calculated enthalpy of formation of all the intermediate phases and the experimental data. The consistencies for all the phases are reasonable except some mismatch exists for Ca₃Zn where the experimental value is more negative than the calculated value. This is probably due to the less accurate vapor pressure measurement followed by [50]. However, the calculations of [59,62] showed very similar results to the present calculation. The calculated enthalpy of mixing in comparison to the calculated curve of [59] over the Ca–Zn liquid phase at 1173 K is shown in Fig. 10. The trend of these two curves is similar however, the results of [59] are more exothermic than the present calculation for the whole composition range.

4.3. Mg–Ca binary system

All the phases except Mg₂Ca compound of the Mg–Ca binary system were reproduced using the same model parameters reported by Aljarrah and Medraj [11]. The intermediate compound Mg₂Ca has the Laves C14 crystal structure which is similar to

MgZn₂. Hence it is decided to remodel Mg₂Ca using the compound energy formalism in order to represent both MgZn₂ and Mg₂Ca Laves C14 phases by one Gibbs energy function in the Mg–Ca–Zn ternary system. The optimized phase diagram of Aljarrah and Medraj [11] is shown in Fig. 11 but with the newly optimized Mg₂Ca Laves phase from the present work.

4.4. Mg–Ca–Zn ternary system

A self-consistent thermodynamic database for the Mg–Ca–Zn system has been constructed by extrapolating the three constituting binaries Mg–Zn, Ca–Zn and Mg–Ca. Three ternary interaction parameters were used in order to achieve consistency with the available experimental data from the literature. The symmetric Kohler geometric model [64] was used for extrapolation since none of the constituent binaries show extreme dissimilarity in their thermodynamic properties. The different ternary compounds reported in the literature were considered during the present optimization.

From Fig. 12, it can be seen that there are six ternary eutectic (E₁–E₆) points, eleven quasi-peritectic (U₁–U₁₁) points, one ternary peritectic (P₁) and eight maximum (m₁–m₈) points present in this system. Information of all the ternary invariant points is summarized in Table 7. The calculated liquidus projection shows reasonable consistency with the experimental results for most of the primary solidification regions except some deviation in the Zn-rich side. This is perhaps due to the fact that, Paris [45] reported two different compounds namely CaZn₁₀ and CaZn₄ in that region. But later investigation proved four other compounds: CaZn₃, CaZn₅, CaZn₁₁ and CaZn₁₃. It is not clear from Paris' results which data points correspond to CaZn₃ and which ones would correspond to CaZn₅. The same applies to the CaZn₁₁ and CaZn₁₃ compounds. Hence in Fig. 12, based on Paris' work [45] one common symbol was used to mark CaZn₃ and CaZn₅ and another one for CaZn₁₁ and CaZn₁₃. It is also worth noting that, assuming the existence of a second ternary compound (Ca₂Mg₅Zn₁₃) during optimization, resulted in a better consistency with the experimental points of Paris [45] and Clark [10]. More details about this assumption in comparison with the other possibilities will be discussed in the following section.

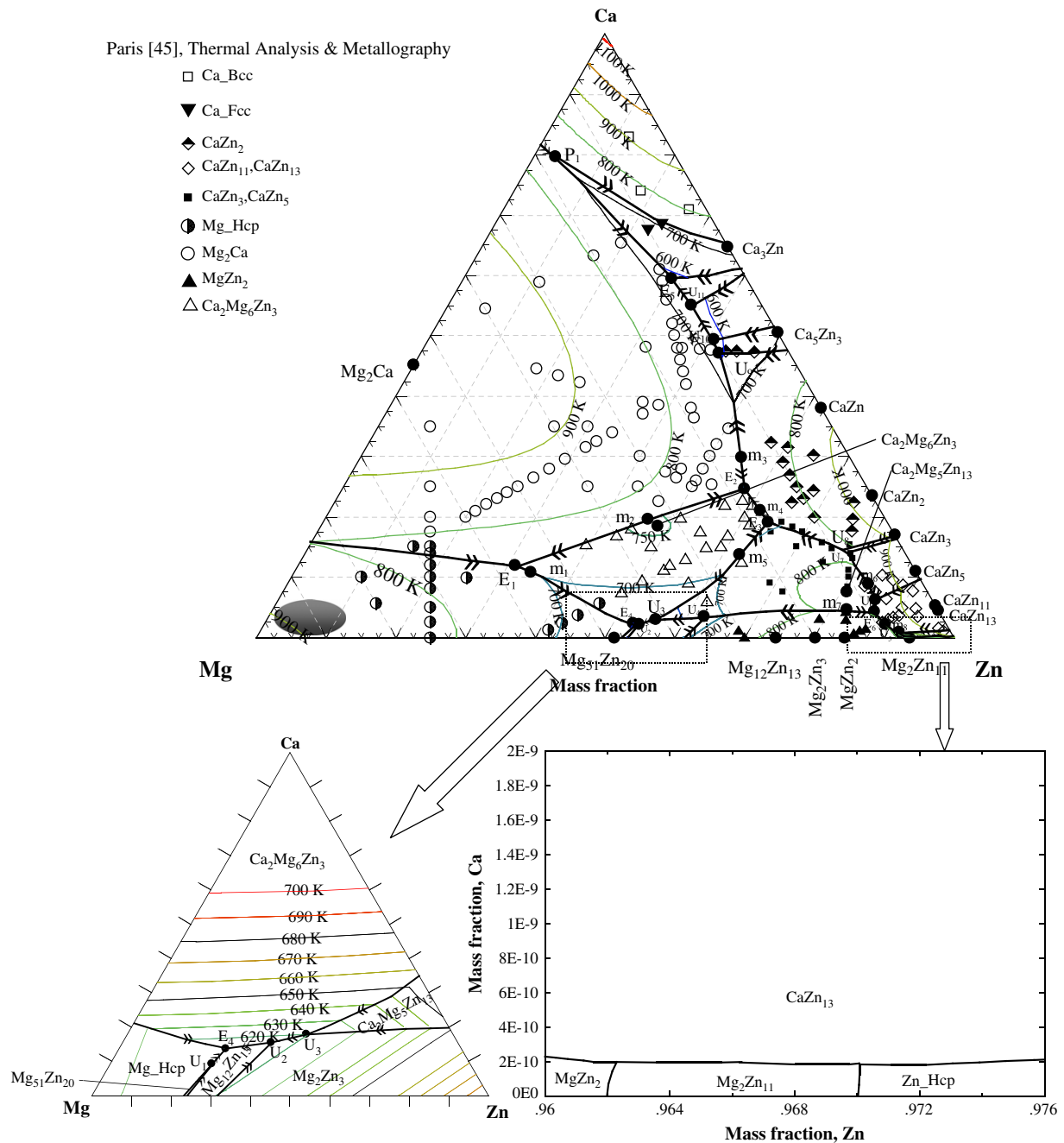


Fig. 12. Calculated liquidus surface of the Mg–Ca–Zn system in comparison with the experimental data of Paris [45]. The shaded area in the Mg-rich region shows the location of the compositions used in [54,55].

4.4.1. The approach followed to include the ternary compounds in the Mg–Ca–Zn system

As mentioned earlier, the experimental data reported in the literature by Paris [45] and Clark [10] regarding the number of ternary compounds in the Mg–Ca–Zn system is self-contradicting. Therefore several scenarios combining these two works were tried in order to find out the most probable description of this system. In this method, the ternary phase diagram was calculated and compared with all the experimental data for the following cases:

- Considering only the compound (Ca₂Mg₅Zn₅) reported by Paris [45]

- Considering only one (Ca₂Mg₆Zn₃) of the two compounds reported by Clark [10]
- Considering only the two ternary compounds (Ca₂Mg₆Zn₃ and Ca₂Mg₅Zn₁₃) reported by Clark [10]
- Considering Paris' compound (Ca₂Mg₅Zn₅) with one of Clark's compounds (Ca₂Mg₅Zn₁₃)

Several vertical sections (Sections V–VII in Fig. 1) which passed through the regions of probable compound formation have been chosen and presented in Figs. 13–16, for the better clarification and comparison.

Fig. 13 illustrates the calculated vertical sections V–VII by considering only the ternary compound reported by Paris [45]. It

Table 7
Calculated four-phase equilibria points and their reactions in the Mg–Ca–Zn system.

Type	Reaction	Composition (wt.%)			Temperature (K)	Reference
		Mg	Ca	Zn		
E ₁	L ↔ Mg_Hcp + Ca ₂ Mg ₆ Zn ₃ + Mg ₂ Ca	55.6	11.5	32.9	701.5	This work [45]
		55.5	16.0	28.5	673.0	
E ₂	L ↔ Mg_Hcp + Ca ₂ Mg ₆ Zn ₃ + CaZn ₂	17.6	24.7	57.7	720.0	This work [45]
		13.5	24.0	62.5	723.0	
E ₃	L ↔ CaZn ₂ + Ca ₂ Mg ₆ Zn ₃ + Ca ₂ Mg ₅ Zn ₁₃	17.1	19.2	63.7	720.0	This work
E ₄	L ↔ Mg_Hcp + Ca ₂ Mg ₆ Zn ₃ + Mg ₁₂ Zn ₁₃	44.5	2.1	53.4	610.0	This work
E ₅	L ↔ Mg ₂ Ca + Ca_Fcc + Ca ₃ Zn	10.5	59.5	30.0	580.0	This work [45]
		8.0	59.0	33.0	592.0	
E ₆	L ↔ Ca ₂ Mg ₅ Zn ₁₃ + MgZn ₂ + CaZn ₁₁	9.1	4.0	86.9	800.0	This work
P ₁	L + Mg ₂ Ca + Ca_Bcc ↔ Ca_Fcc	17.0	78.7	4.3	708.0	This work
U ₁	L + Mg ₅₁ Zn ₂₀ ↔ Mg_Hcp + Mg ₁₂ Zn ₁₃	46.4	1.0	52.6	599.0	This work
U ₂	L + Mg ₂ Zn ₃ ↔ Mg ₁₂ Zn ₁₃ + Ca ₂ Mg ₆ Zn ₃	44.7	1.5	53.8	615.0	This work
U ₃	L + Ca ₂ Mg ₅ Zn ₁₃ ↔ Mg ₂ Zn ₃ + Ca ₂ Mg ₆ Zn ₃	43.7	1.8	54.5	620.0	This work
U ₄	L + MgZn ₂ ↔ Mg ₂ Zn ₃ + Ca ₂ Mg ₅ Zn ₁₃	35.3	2.2	62.5	682.0	This work
U ₅	L + CaZn ₁₁ ↔ MgZn ₂ + CaZn ₁₃	7.9	0.9	91.2	790.0	This work
U ₆	L + CaZn ₅ ↔ CaZn ₁₁ + Ca ₂ Mg ₅ Zn ₁₃	7.8	6.7	85.5	810.0	This work
U ₇	L + CaZn ₅ ↔ CaZn ₃ + Ca ₂ Mg ₅ Zn ₁₃	8.0	14.3	77.7	780.0	This work
U ₈	L + CaZn ₃ ↔ CaZn ₂ + Ca ₂ Mg ₅ Zn ₁₃	8.5	14.8	76.7	770.0	This work
U ₉	L + CaZn ₂ ↔ Mg ₂ Ca + CaZn	10.0	47.4	42.6	598.0	This work
U ₁₀	L + CaZn ↔ Mg ₂ Ca + Ca ₅ Zn ₃	10.0	49.5	40.5	588.0	This work
U ₁₁	L + Ca ₅ Zn ₃ ↔ Mg ₂ Ca + Ca ₃ Zn	10.2	55.2	34.6	580.0	This work
m ₁	L ↔ Mg_Hcp + Ca ₂ Mg ₆ Zn ₃	54.5	10.8	34.7	711.2	This work
m ₂	L ↔ Mg ₂ Ca + Ca ₂ Mg ₆ Zn ₃	34.8	19.3	45.9	776.3	This work
m ₃	L ↔ Mg ₂ Ca + Ca ₂ Mg ₆ Zn ₃	15.6	30.0	54.4	723.7	This work
m ₄	L ↔ CaZn ₂ + Ca ₂ Mg ₆ Zn ₃	17.1	21.0	61.9	722.3	This work
m ₅	L ↔ Ca ₂ Mg ₆ Zn ₃ + Ca ₂ Mg ₅ Zn ₁₃	23.6	13.7	62.7	740.3	This work
m ₆	L ↔ CaZn ₅ + Ca ₂ Mg ₅ Zn ₁₃	8.0	8.8	83.2	834.4	This work
m ₇	L ↔ MgZn ₂ + Ca ₂ Mg ₅ Zn ₁₃	13.4	4.5	82.1	824.7	This work
m ₈	L ↔ MgZn ₂ + CaZn ₁₁	8.6	2.6	88.8	804.9	This work

shows reasonable consistency except some deviation in the region belonging to CaZn₅ especially in Fig. 13(b) and (c) (sections VI and VII) which might be an indication of the presence of a second compound.

By considering one of the two ternary compounds reported by Clark [10] almost similar liquidus curves like the first case have been obtained and demonstrated in Fig. 14. Again the presence of a second ternary phase near the primary solidification region of CaZn₅ especially in Fig. 14(b) and (c) (sections VI and VII) becomes markedly apparent.

Based on the aforementioned observations, it is decided to consider the two ternary compounds reported by Clark [10]. Fig. 15 illustrates the outcome of this consideration through different vertical sections. It can be seen from this figure that these calculated vertical sections are considerably closer to the experimental data points than those calculated without considering the second ternary compound.

Finally, the system was modeled considering two ternary phases where one of them was reported by Paris [45] (Ca₂Mg₅Zn₅) and the other one reported by Clark [10] (Ca₂Mg₅Zn₁₃). Fig. 16 shows the calculated vertical sections in relation to the experimental data. Liquidus curves similar to those in the previous case have been obtained for all the verticals.

There are two other possibilities which can be considered regarding the ternary compounds in this system. One by including only the second compound reported by Clark [10] (Ca₂Mg₅Zn₁₃). Second, considering the compound reported by Paris [45] (Ca₂Mg₅Zn₅) with the first compound reported by Clark [10] (Ca₂Mg₆Zn₃). These scenarios were not pursued because of the following reasons: (1) the presence of the ternary compound Ca₂Mg₆Zn₃ was confirmed by later investigators [54–56], so it should be included in the Mg–Ca–Zn ternary system. (2) Paris' [45] compound and Clark's [10] first compound are similar in composition. Therefore Clark's first compound is thought of as

a replacement of that of Paris and only one of them should be included in the Mg–Ca–Zn phase diagram.

Therefore, among the four feasible cases which were discussed earlier, it can be seen that the last two where two ternary compounds were considered provided better consistency with the experimental points of the ternary phase equilibria than the first two. In the last two feasible scenarios, the second phase (Ca₂Mg₅Zn₁₃) as reported by Clark [10] is common. The only difference between these two cases is the composition of the first ternary compound which is Ca₂Mg₆Zn₃ (reported by Clark [10]) for the third case and Ca₂Mg₅Zn₅ (reported by Paris [45]) for the last one. Clark [10] heat treated the alloys using diffusion couple for almost three weeks and this method proved to be more reliable for phase identification than that of Paris [45] who used thermal and metallographic analyses. In addition, Paris' liquidus curves suggested the presence of the second ternary compound which he was unable to detect. It is also worth mentioning that, the works of Larinova et al. [54] and Jardim et al. [55] mainly concentrated on the primary solidification region of Mg-rich solid solution and the locations of their alloy compositions are shown in Fig. 12. For this reason perhaps they were unaware about the existence of the second ternary phase. Hence more emphasis has been given on the result of Clark [10]. All the other isopleths of Paris [45] shown in Fig. 1 were also reproduced concurrently during optimization considering the two ternary compounds of Clark and found to be consistent.

Fig. 17 shows the calculated isothermal section of the Mg–Ca–Zn system at 608 K where reasonable agreement with the experimental data of Clark [10] was achieved by considering two ternary compounds. Some discrepancy can be observed around the ternary phase Ca₂Mg₆Zn₃ because it was modeled as stoichiometric phase whereas, Clark [10] speculated homogeneity in that phase but he was unable to determine its limits. It can also be seen from the same figure that a small region of liquid phase appears in the

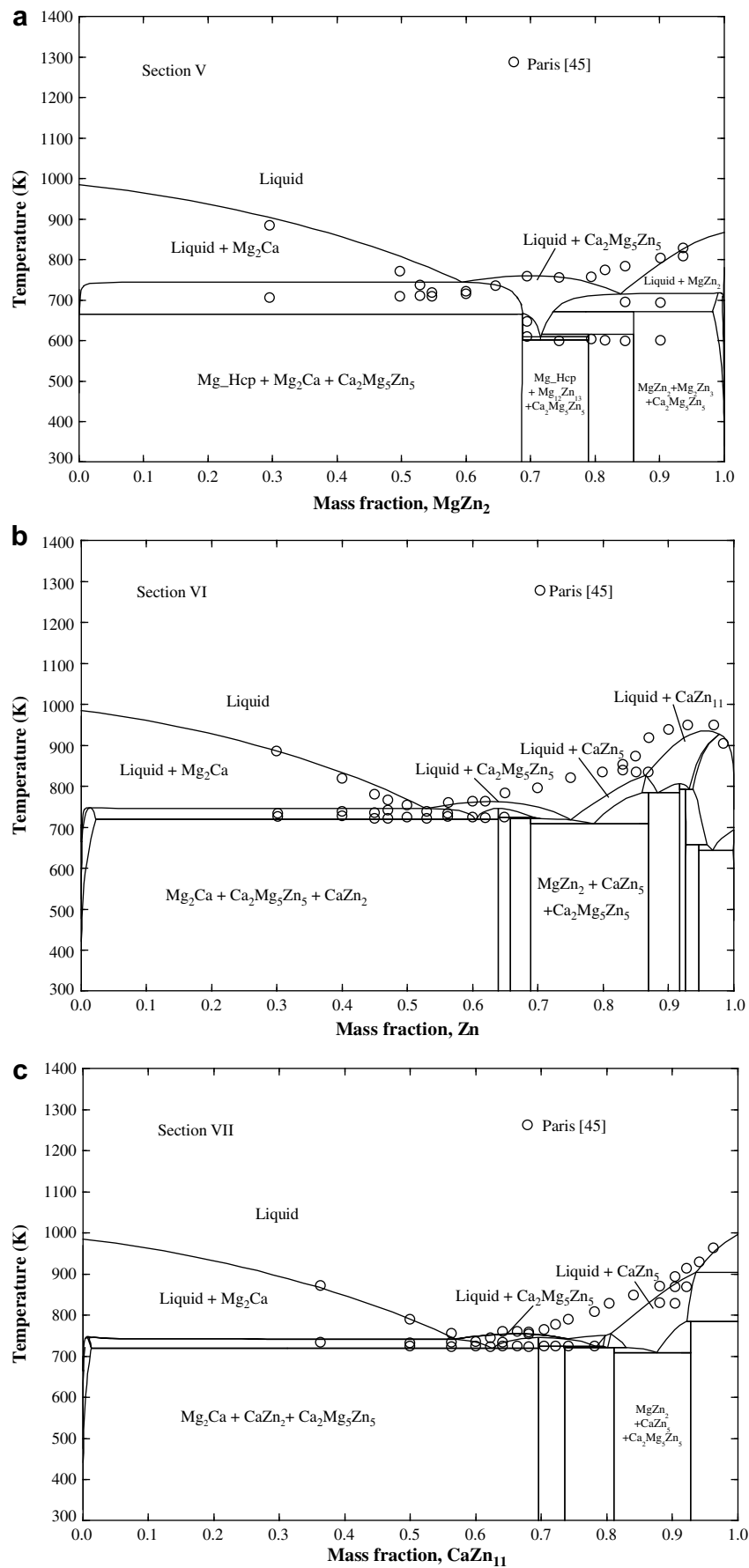


Fig. 13. Calculated isoplethal analysis of sections (a) Mg₂Ca-MgZn₂, (b) Mg₂Ca-Zn and (c) Mg₂Ca-CaZn₁₁ in comparison with the experimental data of [45].

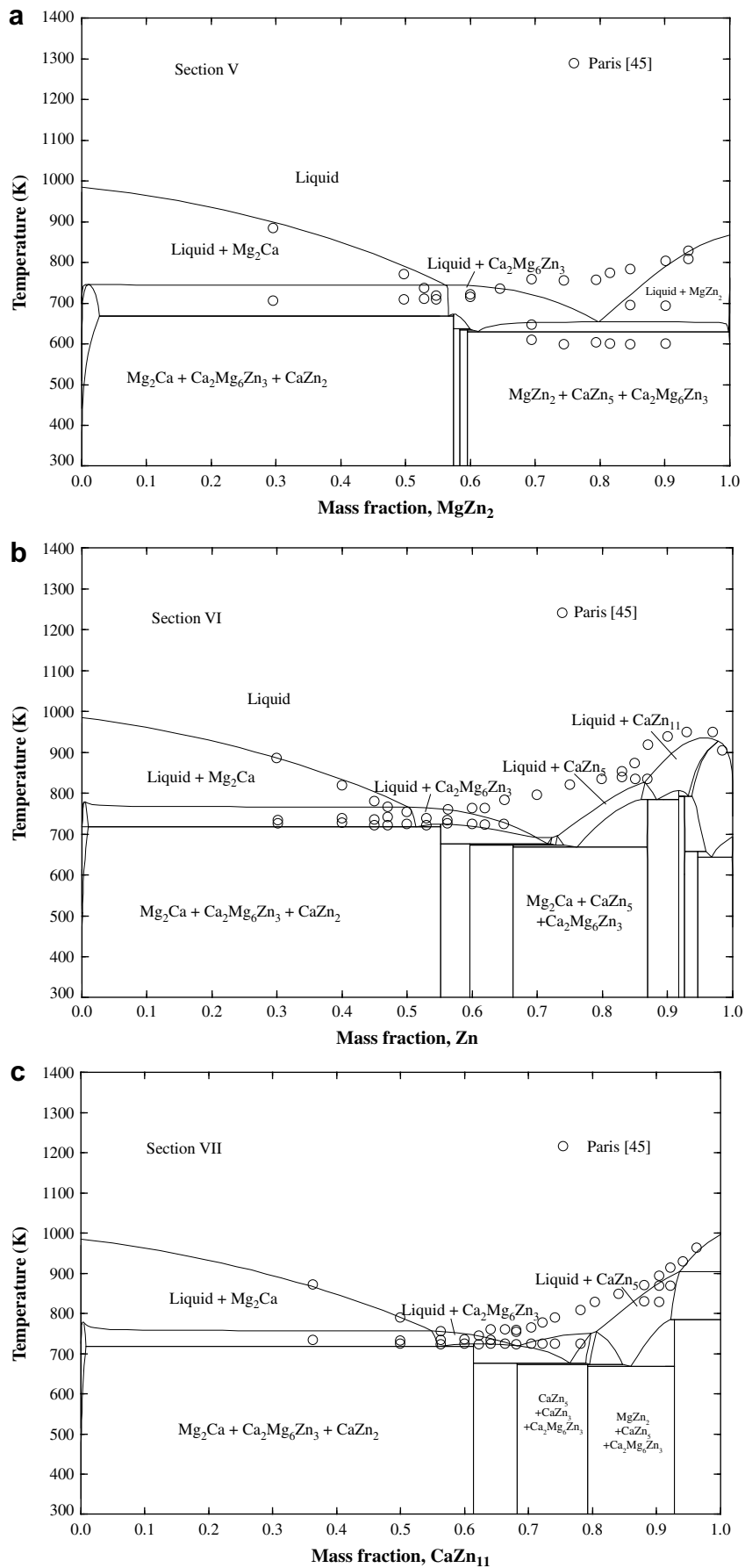


Fig. 14. Calculated isoplethal analysis of sections (a) Mg_2Ca - MgZn_2 , (b) Mg_2Ca -Zn and (c) Mg_2Ca - CaZn_{11} in comparison with the experimental data of [45].

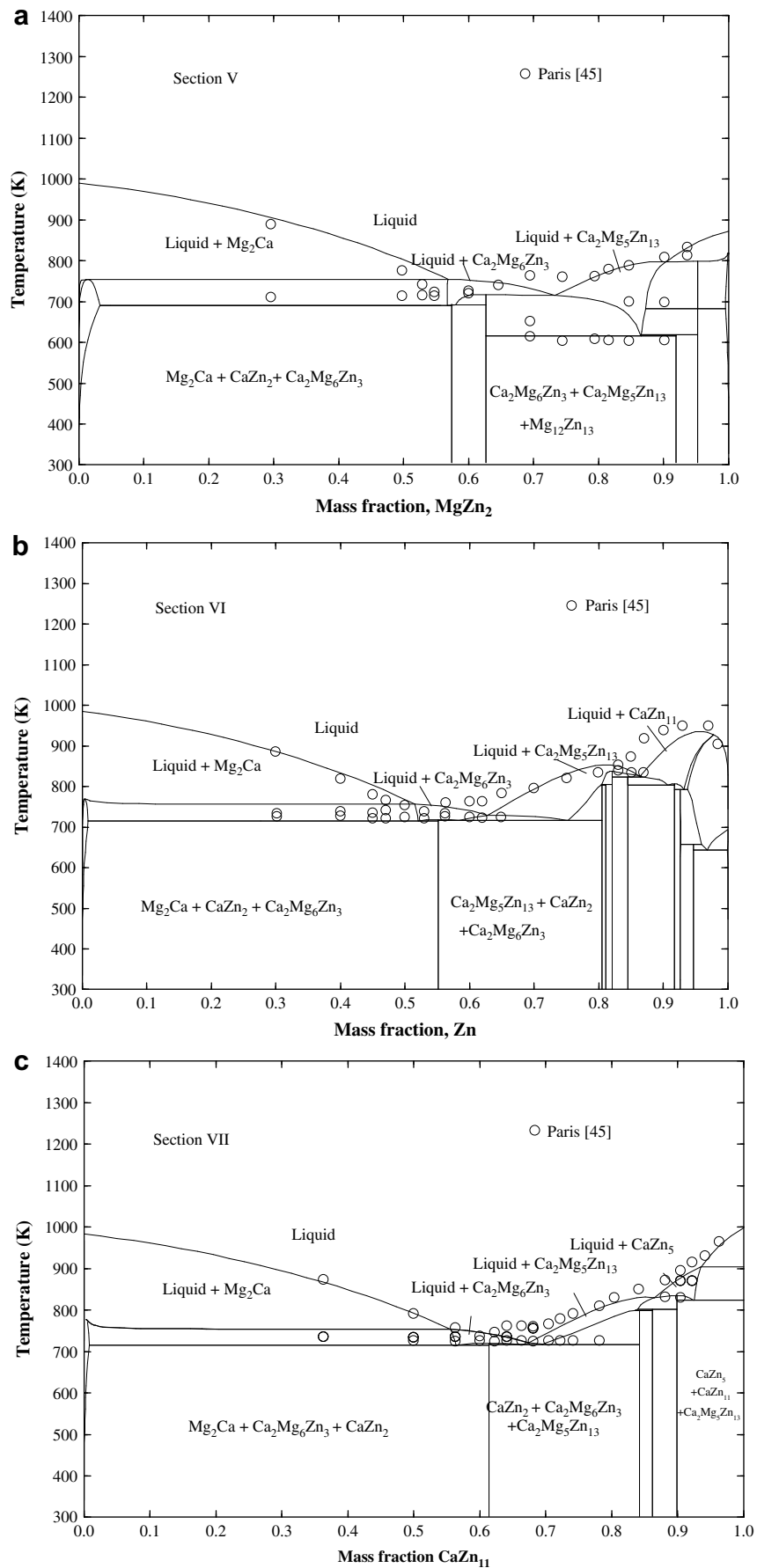


Fig. 15. Calculated isoplethal analysis of sections (a) Mg₂Ca-MgZn₂, (b) Mg₂Ca-Zn and (c) Mg₂Ca-CaZn₁₁ in comparison with the experimental data of [45].

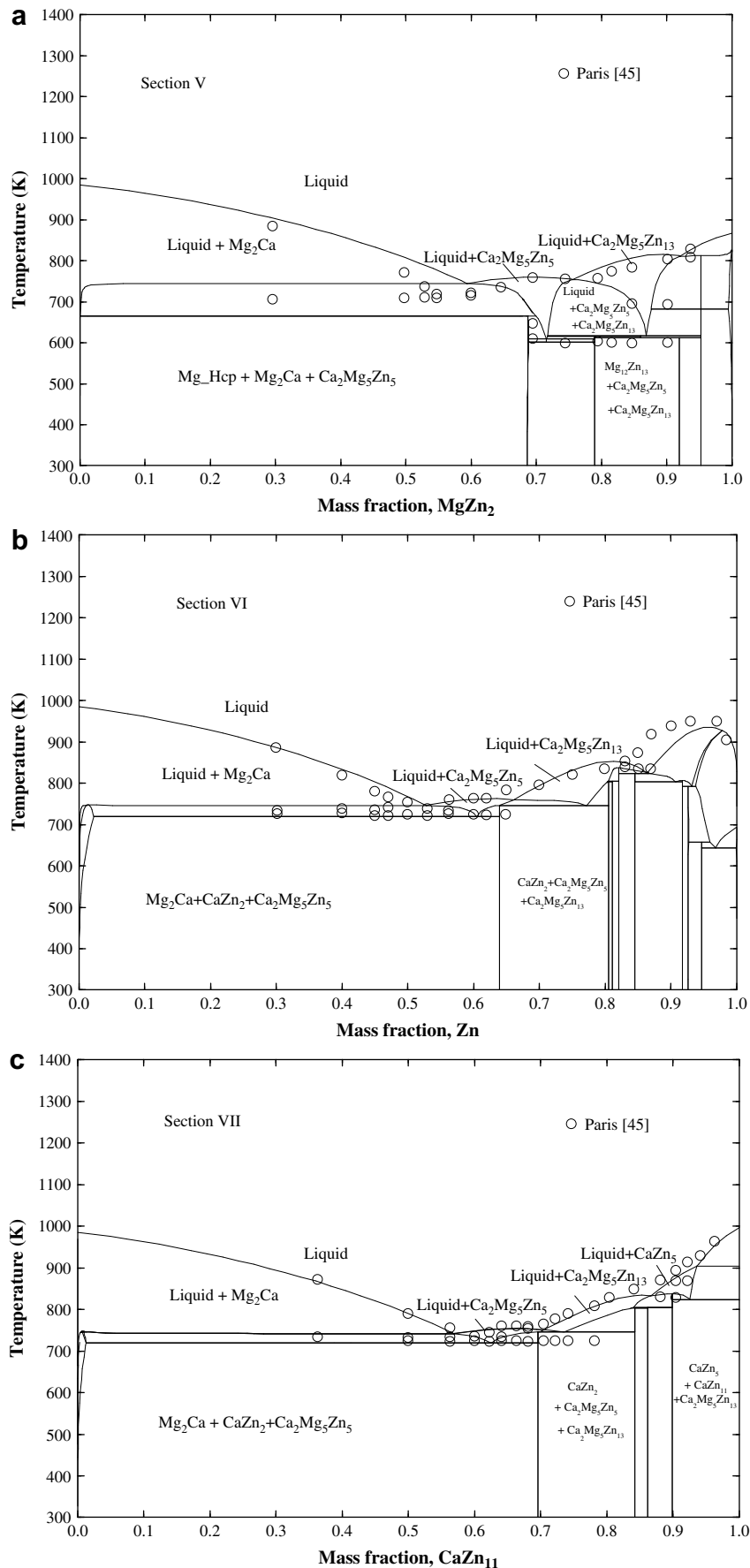


Fig. 16. Calculated isoplethal analysis of sections (a) Mg₂Ca-MgZn₂, (b) Mg₂Ca-Zn and (c) Mg₂Ca-CaZn₁₁ in comparison with the experimental data of [45].

- [23] Clark JB, Rhines FN. Central region of the magnesium–zinc phase diagram. *Journal of Metals* 1957;9:425–30.
- [24] Takei T. The equilibrium diagram of the system magnesium–zinc. Kinzoku-no Kenkyu, Japan Institute of Metals 1929;6:177–83.
- [25] Anderko KP, Klimek EJ, Levonson DW, Rostocker W. Constituent studies on the system magnesium–zinc. *Transactions of the American Society for Metals* 1957;49:778–93.
- [26] Park JJ, Wyman LL. Phase relationships in magnesium alloys, WADC technical report. 57-504, Astia Document No. AD142110; 1957. p. 1–27.
- [27] Higashi I, Shotani N, Uda M, Mizoguchi T, Katoh H. The crystal structure of $Mg_{51}Zn_{20}$. *Journal of Solid State Chemistry* 1981;36:225–33.
- [28] Schmidt W, Hansen M. Solidus and solvus of the magnesium solid solution of magnesium–zinc alloys. *Zeitschrift fur Metallkunde* 1927;19:452–5.
- [29] Grube G, Burkhardt A. The electrical conductivity, thermal expansion and hardness of magnesium–zinc. *Zeitschrift fur Elektrochemie und Angewandte Physikalische Chemie* 1929;35:315–31.
- [30] Schmid E, Seliger H. Investigation of the solid solutions of magnesium. *Metallwirtschaft, Metallwissenschaft, Metalltechnik* 1932;11:409–12.
- [31] Clark JB, Zabdyr L, Moser Z. Mg–Zn: phase diagrams of binary magnesium alloys. Metals Park, OH: ASM; 1988. p. 353–65.
- [32] Agarwal R, Fries SG, Likas HL, Petzow G, Sommer F, Chart TG, et al. Assessment of the Mg–Zn system. *Zeitschrift fur Metallkunde* 1992;83(4):216–23.
- [33] Liang P, Tarfa T, Robinson JA, Wagner S, Ochlin P, Harmelin MG, et al. Experimental investigation and thermodynamic calculation of the Al–Mg–Zn system. *Thermochemica Acta* 1998;314:87–110.
- [34] Redlich O, Kister AT. Thermodynamics of nonelectrolyte solutions, X–Y–T relations in a binary system. *Journal of Industrial and Engineering Chemistry* 1948;40:341–5.
- [35] Pyka H. Untersuchungen zur Thermodynamik glasbildender ternärer Legierungen, Ph.D. thesis, University Stuttgart, Stuttgart, Germany; 1984.
- [36] Agarwal R, Sommer F. Calorimetric investigations of Mg–Zn and Mg–Y liquid alloys. In: Proceedings of eighth national symposium thermal analysis. Bombay, India: Indian Thermal Analysis Society; 1991. p. 249–54.
- [37] Chiotti SP, Stevens ER. Thermodynamic properties of Mg–Zn alloys. *Transactions of the American Society for Metals* 1965;233(1):198–203.
- [38] Moser Z. Thermodynamic properties of dilute solutions of magnesium in zinc. *Metallurgical Transactions* 1974;5(6):1445–50.
- [39] Pogodaev AM, Lukashenko EE. Thermodynamic study of molten magnesium and zinc alloys. *Russian Journal of Physical Chemistry* 1972;46(2):334–9.
- [40] Kozuka Z, Moriyama J, Kushima I. Activity of the component metal in fused binary alloys – Zn–Al and Zn–Mg systems. *Journal of Electrochemical Society of Japan* 1960;28(10):523–6.
- [41] Schneider A, Klotz H, Stendel J, Strauss G. Thermochemistry of magnesium alloys. *Pure and Applied Chemistry* 1961;2:13–6.
- [42] King RC, Kleppa OJ. A thermochemical study of some selected laves phases. *Acta Metallurgica* 1964;12(1):87–97.
- [43] Pedokand TO, Shkol'Nikov SN, Tomazova EV. Thermodynamic study of magnesium–zinc alloys in a solid state. *Tr. Leningr. Politekhn. In-Ta* 1976;348:34–9.
- [44] Donski L. Alloys of calcium with zinc, cadmium, aluminum, thallium, lead, tin, bismuth, antimony and copper. *Zeitschrift fur Anorganische Chemie* 1908;57:185–93.
- [45] Paris R. Ternary alloys. No. 45. Publications Scientifiques et Techniques du minist'ere de L'Air, Ministère de L'Air; 1934. p. 1–86.
- [46] Messing AF, Adams MD, Steunenber RK. Contribution to the phase diagram calcium–zinc. *Transactions of the ASM* 1963;56:345–50.
- [47] Bruzzone G, Franceschi E, Merlo F. M_5X_3 intermediate phases formed by Ca, Sr and Ba. *Journal of the Less-Common Metals* 1978;60:59–63.
- [48] Fornasini ML, Merlo F. $CaZn_3$: a structure with mixed $BaLi_4$ and $CeCu_2$ -like ordering. *Acta Crystallography* 1980;B36:1739–44.
- [49] Itkin VP, Alcock CB. The Ca–Zn system. *Bulletin of Alloy Phase Diagrams* 1990;11(4):328–33.
- [50] Chiotti P, Hecht RJ. Thermodynamic properties of the calcium–zinc system. *Transactions of the Metallurgical Society of AIME* 1967;239:536–42.
- [51] Delcet J, Egan JJ. Thermodynamics of liquid Ca–Zn alloys. *Metallurgical Transactions B* 1978;9B:728–9.
- [52] Clak JB. Joint Committee on powder diffraction standards (JCPDS) card 12-266; 1961.
- [53] Clak JB. Joint Committee on powder diffraction standards (JCPDS) card 12-569; 1961.
- [54] Larinova TV, Park WW, You BS. A ternary phase observed in rapid solidified Mg–Ca–Zn alloys. *Scripta Materialia* 2001;45:7–12.
- [55] Jardim PM, Solorzano G, Sande JBV. Second phase formation in melt-spun Mg–Ca–Zn alloys. *Materials Science and Engineering A* 2004;381(1–2):196–205.
- [56] Jardim PM, Solorzano G, Sande JBV. Precipitate crystal structure determination in melt spun Mg–1.5 wt%Ca–6wt%Zn alloy. *Microscopy and Microanalysis* 2002;8:487–96.
- [57] Brubaker CO, Zi-Kui Liu A. Computational thermodynamic model of the Ca–Mg–Zn system. *Journal of Alloys and Compounds* 2004;370(1–2):114–22.
- [58] Dinsdale AT. Thermodynamic data for the elements. *CALPHAD* 1991;15(4):317–425.
- [59] Spencer PJ, Pelton AD, Kang Y-B, Chartrand P, Fuerst CD. Thermodynamic assessment of the Ca–Zn, Sr–Zn, Y–Zn and Ce–Zn system. *CALPHAD* 2008;32(2):423–31.
- [60] Sommer F. Association model for the description of thermodynamic functions of liquid alloys II. Numerical treatment and results. *Zeitschrift fur Metallkunde* 1982;73(2):77–86.
- [61] Pelton AD, Kang Y-B. Modeling short-range ordering in solutions. *International Journal of Materials Research* 2007;98:1–10.
- [62] Brubaker CO, Zi-Kui Liu A. Computational thermodynamic assessment of the Ca–Zn system. *CALPHAD* 2001;25(3):381–90.
- [63] Okamoto H, Massalski TB. Thermodynamically improbable phase diagrams. *Journal of Phase Equilibria* 1991;12(2):148–68.
- [64] Kohler F. Estimation of the thermodynamic data for a ternary system from the corresponding binary systems. *Monatshefte fur Chemie* 1960;91(4):738–40.
- [65] Wieting J. Crystal structure of $CaZn_2$. *Naturwissenschaften* 1961;48:401.
- [66] Haucke W. The crystal structure of $CaZn_5$ and $CaCu_5$. *Zeitschrift fur Anorganische Chemie* 1940;244:17–22.
- [67] landelli A, Palenzona A. Zinc-rich phases of the rare-earth zinc alloys. *Journal of the Less-Common Metals* 1967;12(5):333–43.
- [68] Ketelaar JAA. The crystal structure of alloys of zinc with the alkali and alkaline earth metals and of cadmium with potassium. *Journal of Chemical Physics* 1937;5:668.
- [69] Vosskühler H. The phase diagram of magnesium-rich Mg–Ca alloys. *Zeitschrift fur Metallkunde* 1937;29:236–7.
- [70] Baar N. On the alloys of molybdenum with nickel, manganese with thallium, and calcium with magnesium, thallium, lead, copper, and silver. *Zeitschrift fur Anorganische Chemie* 1911;70:362–6 (From British Library www.bl.uk, "Ca–Mg (calcium–magnesium)", *Landolt-Bornstein Series IV/5c*, p. 22–25).
- [71] Houghton JL. Alloys of magnesium. Part 6—the construction of the magnesium-rich alloys of magnesium and calcium. *Journal Institute of Metals* 1937;61:241–6.
- [72] Nowotny H, Wormnes E, Mohrnhelm A. Investigation on the Al–Ca, Mg–Ca, and Mg–Zr systems. *Zeitschrift fur Metallkunde* 1940;32:39–42.
- [73] Bulian W, Fahrenhorst E. Solubility of calcium in magnesium. *Metallforschung* 1946;1:70.
- [74] Burke EC. Solid solubility of calcium in magnesium. *Journal of Metals, Transaction AIME* 1955;203:285–6.
- [75] Klemm W, Dinkelacker F. On the behavior of magnesium with calcium, strontium and barium. *Zeitschrift fur Anorganische Chemie* 1947;255:2–12.
- [76] Okamoto H, editor. Binary alloy phase diagrams. 2nd ed. plus updates. ASM; 1996.
- [77] Damms JLC, Villars P, van Vucht JHN, editors. Atlas of crystal structure types for intermetallic phases, vol. 3. Metals Park, OH: ASM International; July 1991. p. 4937–9.